

Heat transfer of a non-Newtonian fluid (Carbopol aqueous solution) in transitional pipe flow

J. Peixinho^{*}, C. Desaubry, M. Lebouché

LEMTA – Laboratoire d'Énergétique et de Mécanique Théorique et Appliquée, 2 Avenue de la forêt de Haye, BP 160, 54 504 Vandœuvre-lès-Nancy, France

Received 23 May 2006; received in revised form 2 February 2007

Available online 13 June 2007

Abstract

An experimental study of the forced convection heat transfer for non-Newtonian fluid flow in a pipe is presented. We focus particularly on the transitional regime. A wall boundary heating condition of heat flux is imposed. The non-Newtonian fluid used is Carbopol (polyacrylic acid) aqueous solutions. Detailed rheology as well as the variation of the rheological parameters with temperature are reported. Newtonian and shear thinning fluids are also tested for comparative purposes. The characterization of the flow and the thermal convection is made via the pressure drop and the wall temperature measurements over a range of Reynolds number from laminar to turbulent regime. Our measurements show that the non-Newtonian character stabilizes the flow, i.e., the critical Reynolds number to transitional flow increases with shear thinning and yield stress. The heat transfer coefficients are given and compared with heat transfer laws for different regime flows. Details when the heat transfer coefficient loses rapidly its local dependence on the Reynolds number are analyzed.

© 2007 Elsevier Ltd. All rights reserved.

1. Introduction

Thermal convection for non-Newtonian fluids in pipe flow is of practical importance in a wide range of process industries such as food sterilization or well cementing. Depending on the process considered, the flow can be laminar or turbulent and in some cases transitional. In laminar regime, relations for the heat transfer coefficient exist in the literature. Most of them are an extension of the L ev eque solution. In turbulent regime, empirical correlations were proposed. However, their domain of validity needs to be confirmed through additional data. In the transitional regime, very few is known on its occurrence, the characteristics of the flow and their influence on the heat transfer.

The transition in pipe flow is very sensitive to the inlet conditions. Indeed, careful conditions can permit laminar flow for very large Reynolds numbers. Most of the studies

(including the present one) use facilities such that the transition is triggered by intrinsic imperfections of the setup. For a Newtonian fluid, from a Reynolds number, Re , greater than approximately 2200, patches of turbulent flow appear abruptly as reported in the detailed study of Wignanski and Champagne [1]. (Here $Re = UD/\nu$ where U is the mean velocity, D is the diameter of the pipe, and ν the kinematic viscosity of the fluid.) Above $Re \approx 3200$, the flow can be considered fully turbulent. In the range $2200 \lesssim Re \lesssim 3200$, the flow regime is considered transitional. The thermal convection in this regime, was studied only by Ghajar and Tam [2]. They measured the local heat transfer coefficient in a horizontal circular straight tube under uniform wall heat flux boundary. The test section is of 6 m long and 1.56 cm inner diameter. The fluids used were distilled water and mixture of distilled water and ethylene glycol. The heat transfer transition region was determined by observing the change in the heat transfer behaviour. Finally, the authors used an asymptotic method similar to Churchill [3] to develop a correlation in the transition region, since the variation of heat transfer coefficient is between two asymptotes.

^{*} Corresponding author. Present address: Fluid Engineering Laboratory, Department of Mechanical Engineering, 7-3-1 Hongo, Bunkyo-ku, Tokyo 113-8656, Japan.

E-mail address: jorge@fel.t.u-tokyo.ac.jp (J. Peixinho).

Nomenclature

a	dimensionless plug size, $a = \frac{r_p}{R} = \frac{\tau_Y}{\tau_w}$	T_m	mean temperature ($^{\circ}\text{C}$)
B	Bingham number, $B = \frac{\tau_Y}{K(U/R)}$	T_w	wall temperature ($^{\circ}\text{C}$)
b	Herschel–Bulkley thermo-dependent parameter ($^{\circ}\text{C}^{-1}$)	U	bulk velocity (m/s)
Br	Brinkman number	u	axial velocity (m/s)
C_p	specific heat ($\text{J kg}^{-1} \text{K}^{-1}$)	x	axial position (m)
D	pipe diameter (m)	X^+	Cameron number $X^+ = \frac{x}{D} \frac{1}{Re}$
f	friction factor, $f = \frac{2\tau_w}{\rho U^2}$	<i>Greek symbols</i>	
Gr	Grashof number	β	thermal expansion coefficient ($^{\circ}\text{C}^{-1}$)
h	heat transfer coefficient ($\text{W m}^{-2} \text{K}^{-1}$)	Δ	themo-dependent heat transfer ratio
Hb	Herschel–Bulkley number $Hb = \frac{\tau_Y}{K(U/R)^n}$	δ	thermal boundary layer thickness (m)
K	constant in the Herschel–Bulkley model (Pa s^{-n})	Θ_w	dimensionless wall temperature
k	constant in the cross model (s)	$\dot{\gamma}$	shear rate (s^{-1})
k'	generalized consistency ($\text{Pa s}^{-n'}$)	$\dot{\gamma}_w$	wall shear rate (s^{-1})
L_T	thermal entrance length (m)	η_w	dynamic viscosity of the fluid at pipe wall ($\text{kg m}^{-1} \text{s}^{-1}$)
L_p	length between the two pressure tappings (m)	λ	thermal conductivity ($\text{W m}^{-1} \text{K}^{-1}$)
m	power law exponent in the cross model	μ	dynamic fluid viscosity ($\text{kg m}^{-1} \text{s}^{-1}$)
n	power law exponent in the Oswald and Herschel–Bulkley	μ_0	zero shear stress dynamic viscosity in the cross model ($\text{kg m}^{-1} \text{s}^{-1}$)
n'	generalized index flow behaviour	μ_{∞}	infinite dynamic viscosity in the cross model ($\text{kg m}^{-1} \text{s}^{-1}$)
N_1	first normal stress difference (Pa)	ν	cinematic fluid viscosity ($\text{m}^2 \text{s}^{-1}$)
p	pressure (Pa)	Π	ratio of the wall axial velocity
Pe	Péclet number, $Pe = RePr$	ρ	fluid density (kg m^{-3})
Pr	Prandtl number, $Pr = \frac{\nu}{\lambda}$	τ	shear stress (Pa)
R	pipe radius (m)	τ_Y	yield stress (Pa)
r	radial location within pipe (m)	τ_{rz}	shear stress in unidirectional shear flow (Pa)
r_p	radius of constant velocity plastic plug (m)	τ_w	wall shear stress (Pa)
Re	Reynolds number for Newtonian fluid, $Re = \frac{\rho U D}{\nu}$	ϕ_w	wall heat flux (W m^{-2})
Re'	generalised Reynolds number, $Re' = \frac{\rho U^{2-n'} R^{n'}}{8^{n'-1} k'}$	φ_N	dimensionless wall axial velocity gradient
Re'_C	critical generalised Reynolds number		
Re_w	wall Reynolds number, $Re_w = \frac{\rho U D}{\mu_w}$		
T_e	entrance temperature ($^{\circ}\text{C}$)		

As indicated previously, in industrial applications, non-Newtonian fluids are frequently used. Viscoplastic fluids are a simple case of non-Newtonian fluids. They possess a yield stress, τ_Y , below which, they either flow as an unshered plug or not flow. Nouar and Frigaard [4] and Frigaard and Nouar [5], using theoretical approaches, demonstrated that the yield stress has a stabilizing effect. This is in qualitative agreement with the experimental observations (e.g. Escudier and Presti [6] and Peixinho et al. [7]). The shear thinning, also, delays transition to turbulence as the experimental results obtained by Pinho and Whitelaw [8] and Escudier et al. [9] indicate. Furthermore, in transitional regime and for a given Reynolds number based on the wall viscosity, it is observed that the shear thinning, reduce the radial and azimuthal velocity fluctuations. This tendency was confirmed recently by Rudman et al. [10], using direct numerical simulation. The influence of these modifications, on the thermal field characteristics, in the situation of heating, was never considered. The objective of this work, is to

provide some experimental data for the heat transfer coefficient, particularly in transitional regime.

1.1. Problem description

We consider the flow of a shear thinning yield stress fluid in a cylindrical pipe. The rheological behaviour of the fluid is assumed to be described by the Herschel–Bulkley model. For unidirectional shear flow with velocity, u , in the x direction, the relationship between the shear stress, τ_{rx} , and the velocity gradient is given as:

$$\tau_{rx} = \text{sgn}\left(\frac{du}{dr}\right) \tau_Y + K \left| \frac{du}{dr} \right|^{n-1} \frac{du}{dr} \iff |\tau_{rx}| \geq \tau_Y, \quad (1)$$

$$\frac{du}{dr} = 0 \iff |\tau_{rx}| < \tau_Y, \quad (2)$$

where K is the consistency and n the flow behaviour index. We assume that at an axial position, say $x = 0$, far from the

inlet, the flow is fully developed and the temperature profile is uniform. From $x = 0$, the wall of the duct is heated with a uniform heat flux. A thermal boundary layer develops along the heating zone with a thickness δ given by:

$$\frac{\delta}{D} = O\left(\frac{x/D}{\varphi_w Pe}\right)^{1/3}, \quad (3)$$

where D is the diameter of the pipe, φ_w a dimensionless wall axial velocity gradient and Pe the Péclet number, $Pe = \rho C_p UD/\lambda$ (the ratio of characteristic time of conduction to that of convection). The relation (3) is based on the Lévêque assumptions and is valid for $(x/D) \leq 0.1 \times (L_T/D) = 0.1 \times Pe$, where L_T is the thermal entrance length. One has to note that generally for shear thinning fluids (with or without yield stress) the Péclet number is very large ($Pe > 10^4$) and therefore, from practical point of view, the thermal boundary layer is considered as very thin along all the heating zone. In addition to this aspect of thermal entrance region, the decrease of the consistency of the fluid near the heated wall induces an acceleration of the fluid near the wall and a deceleration in the central zone due to the conservation of the flow rate. It is clear that we have no longer a true plug zone but a pseudo-plug zone, as the elongational strain rate $\partial u/\partial x$ induced by the deceleration of the fluid remains very weak. The notion of pseudo-plug zone was first introduced by Walton and Bittleston [11] to describe the flow of yield stress fluid in eccentric annular duct.

In the above analysis, the flow is laminar and the Reynolds number is well below a critical value for transition to turbulence. The thermal boundary layer is not disturbed and the laminar thermal convection laws can be used. During the transitional regime, turbulent patches embed in the laminar flow, disturb the heat boundary layer and modify the heat transfer.

1.2. Heat transfer in laminar regime

The forced convection in Bingham fluids in a circular pipe with uniform wall temperature, assuming fully developed laminar flow and thermally developing field (Graetz problem) was considered by Hirai [12] and Wissler and Schechter [13]. Under additional assumptions of constant rheological properties and negligible both axial conduction and viscous dissipation, the energy equation was solved by separation of variables method leading to an eigenvalue problem. After computing the eigenvalues and eigenfunctions, the heat transfer coefficient was determined. As expected, it increases with increasing the yield stress, because of the increase of the wall velocity gradient. This problem was revisited later by Blackwell [14], by computing greater number of eigenvalues to get more precise value of the heat transfer coefficient, particularly near the entrance section. Johnston [15] solved the Graetz problem taking into account the axial conduction term. The energy equation is solved numerically and found that the axial conduction can be ignored when the Péclet number, Pe ,

is greater than 1000. Min et al. [16] extended the Graetz problem by including both axial conduction and viscous dissipation. They showed that the heat transfer characteristics are significantly affected by the viscous dissipation with increasing the yield stress. It is a consequence of increasing of the shear rate. The same tendency was also observed in the situation of uniform wall heat flux (Min and Yoo [17]).

In the foregoing studies, the rheological parameters were assumed independent of the temperature. This assumption can have a significant influence on the heat transfer. Forrest and Wilkinson [18] analysed the thermal convection for Hershel–Bulkley fluids in a duct. The flow was assumed fully developed at the entrance section, and quasi-established at each section of the heated zone because the Prandtl number is assumed very large. Finally, the numerical results were illustrated graphically. As expected, it was shown that a decrease of the consistency near the heated wall induced an increase of the wall shear rate and the heat transfer coefficient. Nouar et al. [19] studied the laminar thermal convection in a heated pipe for Herschel–Bulkley fluids having different yield stresses. They indicated that the effect of the thermo-dependency of the consistency on the heat transfer decreases when the plug zone radius increases. Actually, the modification of the heat transfer coefficient by the thermo-dependency of the consistency (effective viscosity in the general case) depends on the temperature difference between the wall and the edge of the thermal boundary layer, which is controlled by the wall shear rate. The full problem of simultaneous development of velocity and temperature profiles with thermo-dependent rheological parameters was solved numerically by Soares et al. [20].

When the length of the heated duct is sufficiently long, free convection can become significant and has to be taken into account. Very few authors deal with this aspect of the problem. Patel and Ingham [21,22] considered the situation of the fully developed mixed convection in vertical plane channel and in a vertical eccentric annulus. They determined the different flow configuration with respect to the ratio Grashof/Reynolds. Recently, Nouar [23] analyzed the mixed convection for Herschel–Bulkley fluid in the thermal entrance region of a horizontal duct heated with a constant heat flux. Rigorous analytic expressions of the modification of the heat transfer coefficient by the free convection were derived.

1.3. Heat transfer in transitional and turbulent regime

To our knowledge, there is practically no information in the literature on the heat transfer for non-Newtonian fluids in the transitional regime. We have found only one paper due to Thomas [24]. The author studied the heat transfer in a duct for a non-Newtonian aqueous thorium oxide suspensions. The rheological behaviour of the suspension is described by a Bingham model. A global heat transfer coefficient is determined from the steam condensation at the pipe wall and at different Reynolds numbers based on the

plastic viscosity. The author observed that except for the displacement in critical Reynolds numbers due to the non-Newtonian character of the slurry, the thorium oxide suspension heat transfer coefficients are very similar to Newtonian heat transfer data.

Under fully developed turbulent flow conditions, it is generally considered that the influence of visco-plasticity on heat transfer can be taken into account by using the plastic viscosity. In other words, at high Reynolds numbers, the Herschel–Bulkley fluid behaves as a power law fluid. Yoo [25] presented an empirical correlation for predicting turbulent heat transfer for purely viscous non-Newtonian fluids:

$$Nu = 0.0152Re_w^{0.845}Pr_w^{-1/3}, \tag{4}$$

where Nu is the Nusselt number. The Prandtl number Pr_w and the Reynolds number Re_w are based on the actual wall viscosity. The relation (4) was recommended in the ranges $0.2 \leq n \leq 0.9$ and $3 \times 10^3 \leq Re_w \leq 9 \times 10^4$. Actually, at high shear rates, the viscoelastic character of the shear thinning fluids becomes important. This is characterized by large value of the first normal stress difference compared to the shear stress. However, this effect does not modify significantly the prediction of (4). In contrast, some dilute polymer solutions exhibiting strong elongational viscosity, experience substantial decrease of heat transfer as compared to Newtonian fluids. In addition, for these fluids, the thermal entrance length in turbulent regime is as long as 400–500 pipe diameters.

1.4. Motivation of the present study and its position with respect to the literature

It is clear from this brief literature review, that there is a serious lack of data concerning the heat transfer in transitional regime. The main objective of this work is to provide experimental data on the heat transfer in transitional

regime for non-Newtonian fluids and to analyze how it is modified by the fluid rheology.

This paper is organized as follows. The experimental facility is described in Section 2 together with the instrumentation. The rheological characteristics of the fluid are given in Section 3. Results of pressure and temperature measurements are given in Section 4. In Section 5, a summary of relevant results and practical significance are presented as a conclusion.

2. Experimental setup and instrumentation

A schematic diagram of the flow loop is shown in Fig. 1. The flow is provided by an eccentric rotor pump (PCM Moineau) (3) from a 150 l capacity tank (1). The pump flow rate can be set between 3×10^{-4} and 7.5×10^{-3} m³/s. At the inlet of the pipe, a grid (7) prevents the swirl flow and favors homogeneous turbulence. A 50 l pressurized tank (6) and anti-vibration coupler (2), located after the pump outlet, act to reduce pulsations in the fluid flow before the entrance of the pipe. The whole pipe is 5.5 m long and 30 mm diameter. It can be divided into three parts. The first part is 1.2 m long and is devoted to the development of the flow. The second part is the heating zone (8). It is six 0.36 m long copper tubes around which a coaxial heated wire (Thermocoax) is wound. Electrical current passes through the wire and generate (by Joule effect) an uniform heat flux along 2.16 m. The maximum heat flux (measured using a wattmeter (AOIP)) is 20 kW/m². All the copper tubes are isolated using an air envelope in (Plexiglass) tube in order to limit the heat losses. The third part 1.8 m long transparent (made of Plexiglass) is used for pressure and flow rate measurements.

An electromagnetic flowmeter (11) ends the test section. For a given flowrate, the total error upon the mean velocity (taking into account the variability of the pump, the flowmeter error, the diameter error) is estimated from 2% to

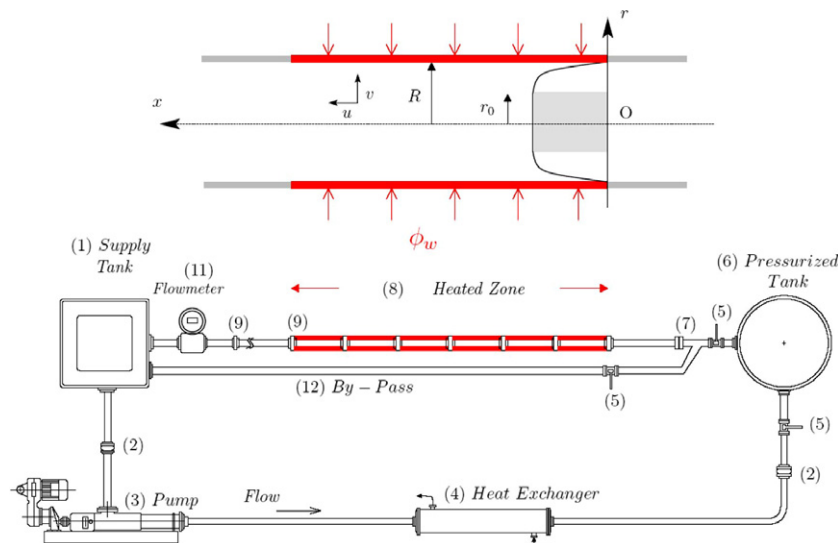


Fig. 1. Schematic diagram of the pipe-flow facility and velocity profile.

3%. Two pressure tappings of 4 mm internal diameter (9) are located at 3.9 and 5.1 m from the inlet of the test section. The tappings are connected to cylindrical chambers, then to tubing which are filled with deionized water and finally to the pressure transducer (Druck). The accuracy of the transducer is estimated to be better than 0.25% of the full range of measurement (0–10 mbar). The cylindrical chambers improve the pressure measurement (especially for yield stress fluid) making the total error about 1%. The Fanning friction factor f measured from a pressure drop Δp between the two pressure tappings distant of L_p is defined by:

$$f = \frac{2\tau_w}{\rho U^2}, \quad (5)$$

where $\tau_w = R\Delta p/2L_p$ is the wall shear stress and ρ is the density of the fluid.

The entrance temperature of the pipe is controlled by a 20 kW tubular heat exchanger (4) using a thermocouple located in the supply tank (1). Temperature measurements in the heated zone (8) proceeds as follow: each heated 0.36 m long element possesses eight thermocouples. Five of the thermocouples are regularly spaced along a top line allowing wall temperature measurements along the top wall. Besides, in a section at the middle of the 0.36 m tube, three supplementary thermocouples are located at 90° each from the other in order to check if natural convection has to be considered. All the 48 thermocouples along the heated zone plus one thermocouple at the entrance of the pipe are linked to a thermal measurement station (Solartron Logger 3430 from Schlumberger). Temperature readings were obtained and averaged over several minutes in the steady state. The precision in temperature measurement is 0.2 °C. The local Nusselt number, Nu , is defined by

$$Nu = \frac{hD}{\lambda} \text{ with } h = \frac{\phi_w}{T_w - T_m}, \quad (6)$$

where h is the heat transfer coefficient, ϕ_w the wall heat flux, T_w the local wall temperature and T_m is the bulk temperature of the fluid at a given section: $T_m = (2\phi_w/\rho UR C_p)x + T_e$ where ρ is the fluid density, C_p the specific heat, x the position from the inlet of the heating zone and T_e the entrance temperature.

3. Tested fluids

Three kinds of fluids are used: (i) a yield stress fluid, (ii) a shear thinning fluid and (iii) a Newtonian fluid as a reference.

- Aqueous polymer solution of 0.2 wt.% Polyacrylic acid grade 940 (Carbopol) from B. F. Goodrich (molecular weight 2.1×10^6 g/mol).
- Aqueous polymer solution of 2 wt.% sodium Carboxy-MethylCellulose grade 7M1C (CMC) from Hercules Aqualon (molecular weight 0.3×10^6 g/mol).
- Glucose syrup 76% from Cerestar.

These fluids are used because they are optically transparent, nontoxic and stable. Aqueous solution of Carbopol and CMC are prepared by mixing powder into deionized water. After that, the Carbopol solution is neutralized using sodium hydroxide. A gelification process accompanies this neutralization. To prevent bacteriological degradation of the fluids, a small amount of formaldehyde is added.

The rheological characteristics of the tested fluids are determined using a controlled stress rheometer (AR2000 from TA Instruments) with a steel 0.5° cone/40 mm plate and truncation of 15 μ m. The rheometer is thermo regulated.

The shear viscosities vs. shear rate for the 0.2% Carbopol, the 2% CMC and the glucose syrup is presented in Fig. 2. The tests were performed for a shear rate range similar to that encountered in the pipe flow (0.1–4000 s^{-1}). The experimental data for the 0.2% Carbopol are fitted by the Herschel–Bulkley model according to Roberts and Barnes [26] and Kim et al. [27]. The shear stress τ is given by the relation (1) and (2). For the 2% CMC solution, two regions can be distinguished depending on the shear rate: a Newtonian region for low shear rate and a transition region which can be described by an Ostwald model. According to Escudier et al. [28], the rheological behaviour can be well described by the Cross model: $\mu = \mu_\infty + (\mu_0 - \mu_\infty)[1 + (k\dot{\gamma})^m]^{-1}$, where μ_0 and μ_∞ are the viscosities at zero and infinite shear rate and k is a constant time of the fluid.

Fig. 3 presents the evolution of the rheological parameters of the Herschel–Bulkley model for a 0.2% Carbopol solution as a function of the temperature. These data are consistent with previous results from Naïmi et al. [29], Loulou et al. [30], and Nouar et al. [19] showing the Carbopol solution is thermo-dependent essentially through the consistency. Forrest and Wilkinson [18] argued that the yield stress is mainly dependent on a mechanical loading of the fluid which is essentially temperature independent. The thermo-dependency parameter (of the consistency), $b = 0.011^\circ C^{-1}$ and decreases with polymer concentration [19]. For comparison, $b \approx 0.02^\circ C^{-1}$ for water.

According to Barnes [31], any shear thinning fluid would exhibit some elastic behaviour. Indeed, Escudier et al. [28] and Kim et al. [27] performed oscillations tests for CMC and Carbopol solution respectively and measured the storage modulus and their sensitivity to preparation protocol and temperature. Another test to characterize the elasticity of a fluid is the measurement of the first normal stress difference, N_1 , as shown in Fig. 4. Our measurements cannot allow to observe a clear trend in the evolution of N_1 vs. the temperature. It is interesting to note, from Fig. 4, that at high shear rate ($\dot{\gamma} \gtrsim 500 s^{-1}$) the 0.2% Carbopol and the 2% CMC have similar elastic properties. Furthermore, they also exhibit similar shear thinning behaviour according to Fig. 2. Consequently, during the flow in the pipe, the only difference between the two solutions is the existence of a plug region.

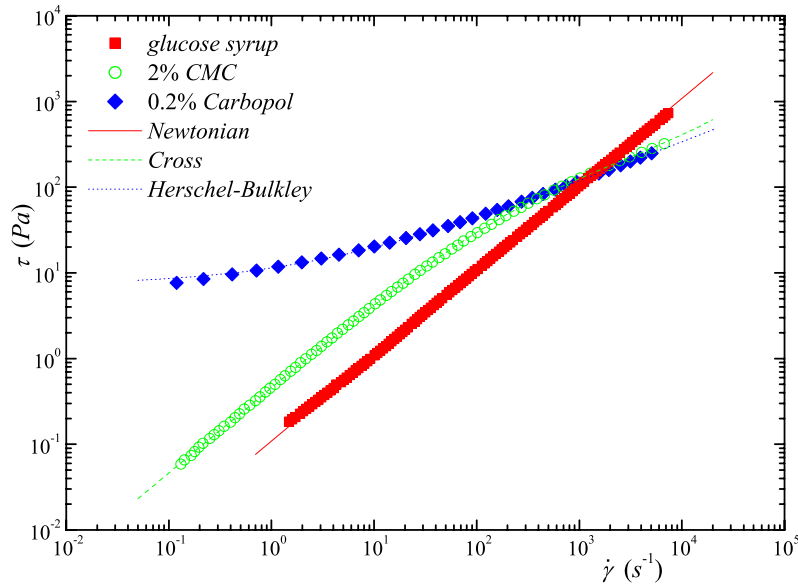


Fig. 2. Shear stress vs. shear rate. The viscosity of the glucose syrup is $\mu = 0.1 \text{ Pa s}$. The behaviour of the 2% CMC solution is described by the Cross model (with $\mu_0 = 0.46 \text{ Pa s}$, $\mu_\infty = 13.6 \text{ mPa s}$, $k = 4.75 \text{ ms}$ and $m = 0.71$) and the 0.2% Carbopol solution by the Herschel–Bulkley model (with $\tau_Y = 7.2 \text{ Pa}$, $K = 4.3 \text{ Pa s}^n$ and $n = 0.47$). The measurements were carried out at $T = 20 \text{ }^\circ\text{C}$.

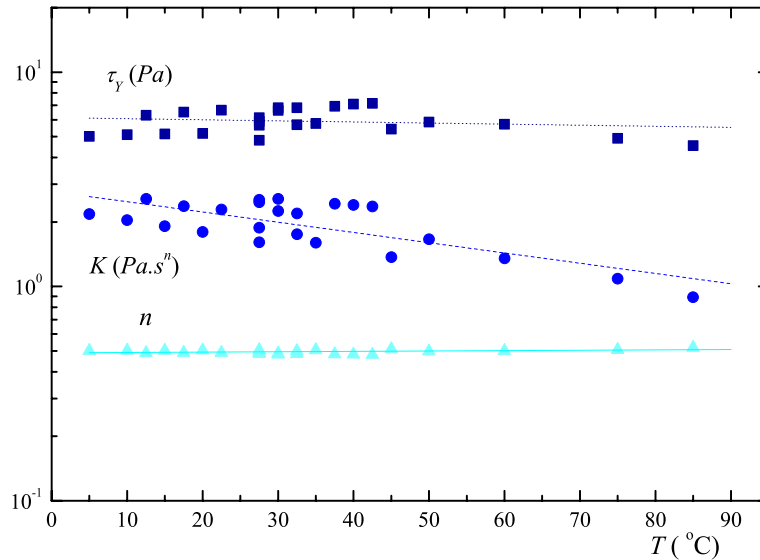


Fig. 3. Evolution of τ_Y , K , and n (constants of the Herschel–Bulkley model) for 0.2% Carbopol solution as a function of the temperature T . The fits are: $\tau_Y = 6.14 \text{ Pa}$, $n = 0.49$ and $K = 2.77 \exp(-0.011 T)$ (K in Pa s^n and T in $^\circ\text{C}$).

Equally important, it is a common practice to consider that the thermo–physical properties of the fluid are those of the solvent (water in our case) at the local mean temperature of the flow, since the concentration of polymers in the aqueous solution is weak. For non-Newtonian fluids, this can be supported by the studies of Lee et al. [32] and Loulou et al. [30] who performed measurements of thermo–physical properties of non-Newtonian fluid and then predict a maximum error on heat coefficient about 2%. Another remark is that the natural convection and viscous dissipation are not considered in this study. It can be shown using scaling analysis or experimental maps (like the one by Gahjar and Tam [2]) that the Grashof number,

Gr , which governs the free convection, is about 10^{-4} . The Brinkman number is also very small (it is about 10^{-3}) and therefore the viscous dissipation can be neglected.

4. Results and discussion

The non-Newtonian fluid flow can be characterized by the generalized Reynolds number, Re' , introduced by Metzner and Reed [33] and defined by $Re' = 16/f$. It is particularly adequate in the laminar regime, given the universality of the $f-Re$ relationship, and consequently it is also widely used to define transition. The expression of Re' in

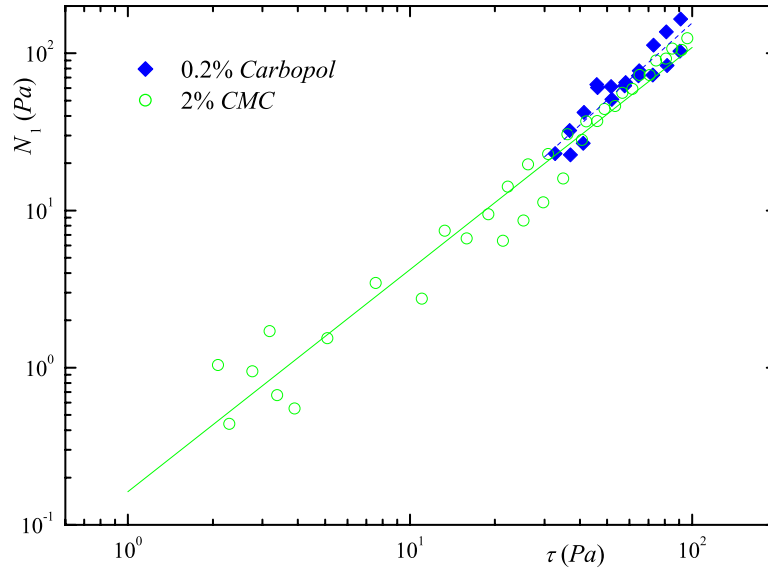


Fig. 4. First normal stress difference vs. shear stress. The lines are power law models: $N_1 = 0.16\tau^{1.4}$ and $N_1 = 0.08\tau^{1.6}$, respectively for the 0.2% Carbopol and the 2% CMC solutions. Measurements carried out at $T = 20^\circ\text{C}$.

the case of a Poiseuille flow of Herschel–Bulkley fluid is given in Appendix A.

The results section is divided in four parts. The first part gives and compares the critical conditions to transition for the fluids used. The second part is dedicated to the laminar heat transfer and confirms previous findings. The measurements of the heat transfer coefficient in transitional and turbulent regimes are given and analyzed in the third part.

4.1. Isothermal flow

The experimental evolution of the friction factor, f , as function of Re' for the three fluids is shown in Fig. 5. In

laminar regime, our measurements follow the relation $f = 16/Re'$. Then, increasing Re' , the measurements for the glucose syrup depart from the laminar law at $Re = 2100$. In the same experimental conditions, the measurement for the 2% CMC solution depart at $Re' = 2500$ and for the 0.2% Carbopol solution at $Re' = 2700$. The non-Newtonian solutions have similar elastic properties as well as shear thinning behaviour. Therefore, it can be concluded that the increase of the critical Reynolds number Re'_C for the Carbopol solution by comparison with CMC solution is due to the presence of the plug zone. Here, it was difficult to separate the influence of shear thinning from that of elasticity on Re'_C . However, the results

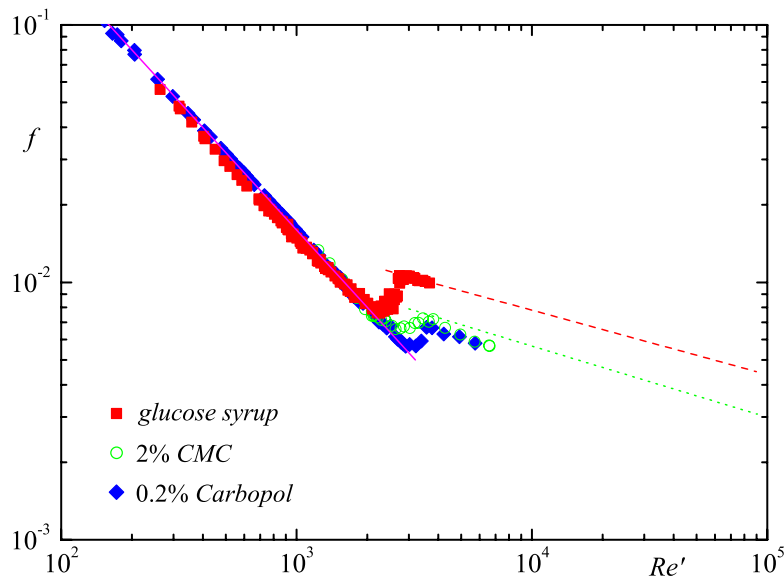


Fig. 5. Friction factor f vs. Reynolds number vs. Re' . The viscosity of the glucose syrup is $\mu = 50\text{ mPa s}$. The behaviour of the 2% CMC solution is described by the Cross model (with $\mu_0 = 67.1\text{ mPa s}$, $\mu_\infty = 4.28\text{ mPa s}$, $k = 1.12\text{ ms}$ and $m = 0.68$) and the 0.2% Carbopol solution by the Herschel–Bulkley model (with $\tau_Y = 6.3\text{ Pa}$, $K = 2.2\text{ Pa s}^n$ and $n = 0.5$). Measurements carried out at $T = 20^\circ\text{C}$.

obtained by Pinho and Whitelaw [8], Park et al. [35], Escudier and Presti [6] indicate that the shear thinning contributes to the flow stability. Concerning the plug zone, it is believed that in the early stage of transition, it is destroyed progressively by the additional shear stresses arising from the disturbance. In the turbulent regime, the experimental results are slightly below Dodge and Metzner expression [33], indicating a weak “elastic” drag reduction.

4.2. Laminar heat transfer

For all the experimental tests, the temperature difference between the top and the bottom did not exceed 1°C. Thus,

the free convection is weak and can be neglected, i.e., the forced convection is the dominant mechanism. Furthermore, the Péclet number was sufficiently large, $Pe > 10^4$, so that the temperature variations are confined in a thin layer (thermal boundary layer) adjacent to the heated wall, along all the heating zone. Indeed, a scaling analysis of the energy equation shows that the magnitude order of the thermal entrance length, L_T , is given by $L_T/R = O(Pe)$. In our experiments, the length of the heating zone is less than 1% of L_T . Adopting the L ev eque assumption, i.e., linear velocity profile inside the thermal boundary layer, and using the energy equation, it can be shown [36,37] that:

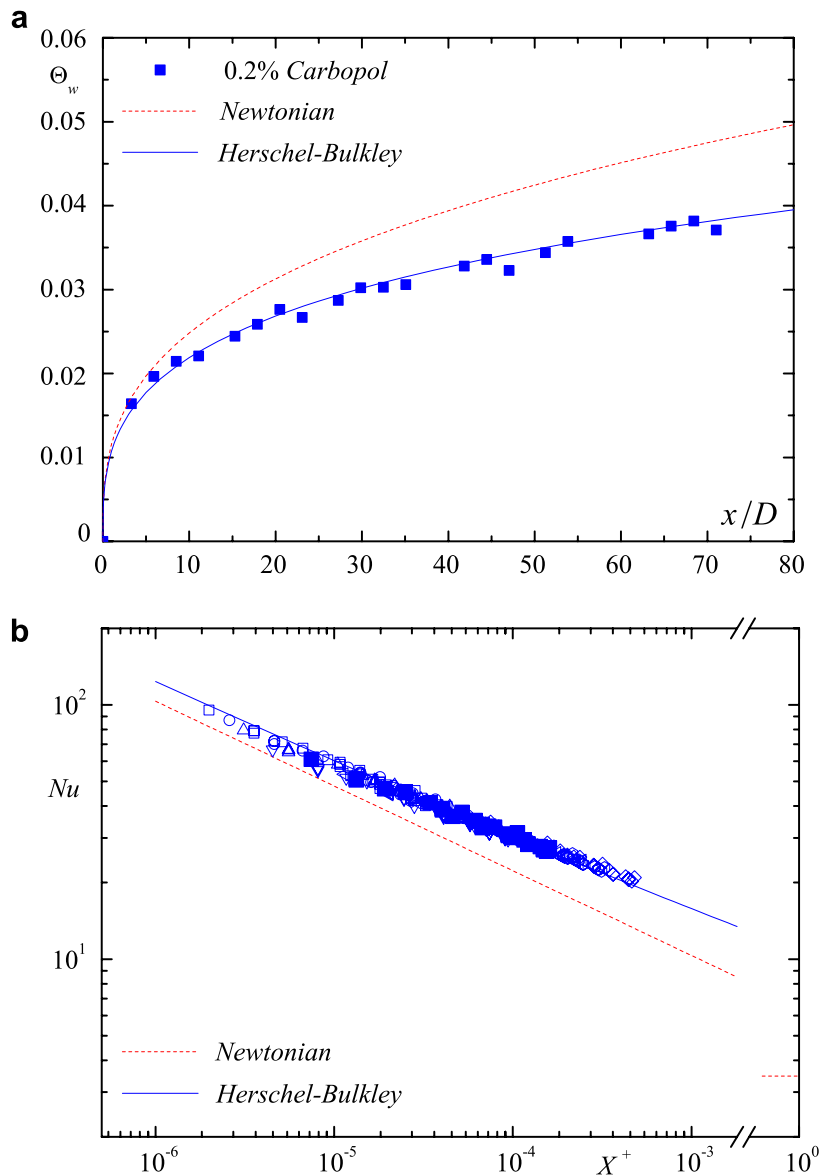


Fig. 6. Heat transfer for 0.2% Carbopol solution in laminar flow. A constant heat flux is imposed at the wall $\phi_w = 15.5 \text{ kW m}^{-2}$. The behaviour of the fluid is described by the Herschel–Bulkley model with $\tau_Y = 7 \text{ Pa}$, $K = 3.1 \text{ Pa s}^n$, $n = 0.45$ and $b = 0.005 \text{ }^\circ\text{C}^{-1}$: (a) Θ_w vs. (x/D) , with $Re' = 200$, $Hb = 0.23$, $a = 0.1$, $Pr' = 2200$, $\Pi = 1.4$ and $1 \leq \Delta \leq 1.9$. The continuous and dotted lines represent the relation (11) for thermo-dependent Herschel–Bulkley fluid and nonthermo-dependent Newtonian fluid, respectively; (b) Nu vs. (X^+) , additional results (empty symbols) covering a large range of X^+ were obtained for Re' from 35 to 1200 and Δ up to 2.7. The continuous and dotted lines represent the relation (7) for thermo-dependent Herschel–Bulkley fluid and nonthermo-dependent fluid, respectively.

$$Nu = \frac{hD}{\lambda} = 2.71 \left(\frac{9X^+}{\varphi_w} \right)^{-1/3}, \tag{7}$$

where $X^+ = (x/D)/Pe$ is a dimensionless axial position and φ_w is a dimensionless wall shear rate: $\varphi_w = [\partial(u/U)/\partial(r/R)]_w$. It can be expressed as a function of the Newtonian wall shear rate $\varphi_{w,newt}$ (with constant viscosity), via two correction factors Π and Δ which represent the effects of non-Newtonian behaviour and thermo-dependency of the consistency respectively:

$$\varphi_w = \frac{\varphi_{w,cp}}{\varphi_{w,newt}} \frac{\varphi_{w,vp}}{\varphi_{w,cp}} \varphi_{w,newt} = \Pi \Delta \varphi_{w,newt}. \tag{8}$$

The subscripts vp and cp mean variable (thermo-dependant) consistency and constant consistency. In the situation of constant consistency, the ratio of the wall shear rate to the

one that would be obtained for a Newtonian fluid at the same flow rate is straightforwardly derived from the expression of the fully developed velocity profile in Appendix A:

$$\Pi = \frac{\varphi_{w,cp}}{\varphi_{newt}} = \frac{1}{4} \left[\frac{Hb(1-a)}{a} \right]^{1/n}. \tag{9}$$

Concerning the expression of Δ , it can be obtained by assuming that for large Pr and $X^+ \ll 1$, the dependence of the wall shear stress with the axial position can be neglected [38,39]:

$$\begin{aligned} \Delta &\approx \left[\frac{K_{r=R,x=0}}{K_{r=R,x}} \right]^n = \exp[b(T_w - T_c)/n] \\ &\approx 1 + \frac{b(T_w - T_c)}{n}. \end{aligned} \tag{10}$$

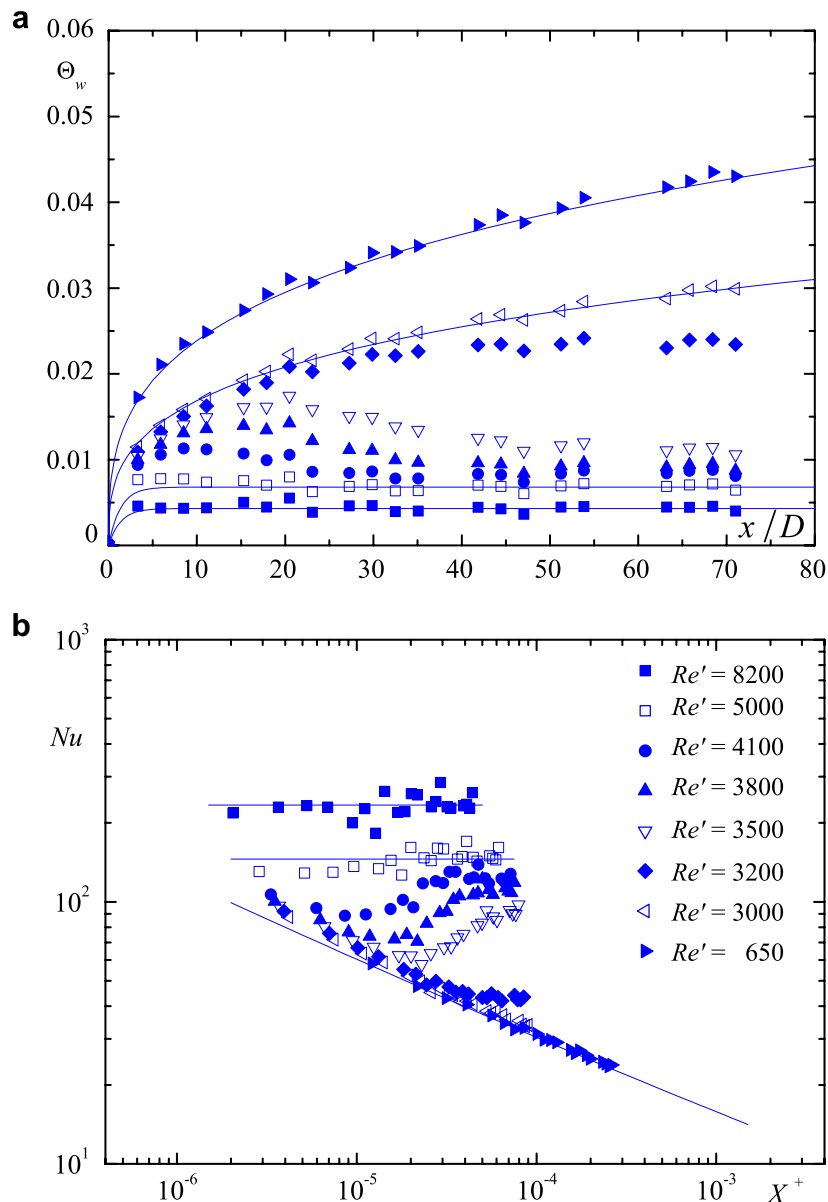


Fig. 7. Heat transfer for 0.2% Carbopol solution. (a) $\Theta_w(x/D)$ and (b) $Nu(X^+)$. The behaviour of the 0.2% Carbopol solution is described by the Herschel–Bulkley model (with $\tau_Y = 7$ Pa, $K = 3.1$ Pa s n , $n = 0.45$ and $b = 0.005$ °C $^{-1}$). The wall boundary condition is a constant heat flux ($\phi_w = 15.5$ kW m $^{-2}$). The lines are fits to guide the eyes.

The temperature difference ($T_w - T_c$) is calculated at a first approximation, using the L ev eque solution with constant consistency:

$$\Theta_w = \frac{T_w - T_c}{\phi D / \lambda} = 1.536 \left(\frac{X^+}{\phi_w} \right)^{1/3}, \quad (11)$$

Having Δ , ϕ_w and Θ_w are recalculated. The convergence is reached practically after two iterations. The Nusselt number is then determined using (7) combined with ((8)–(11)).

This model is confronted to experimental measurement for 0.2% Carbopol solution in Fig. 6a where Θ_w is plotted as a function of x/D . There is a good agreement between the model and the experiment. In Fig. 6b, the same data and additional results for different Re' are represented on the form Nu vs. X^+ . Finally, we validate again this model, which predicts the increase of the heat transfer by the non-Newtonian character of the fluid and the thermo-dependency of the consistency.

4.3. Transitional and turbulent heat transfer

In transitional regime, patches of disordered fluid motion appear, perturb the thermal boundary layer and therefore modify the heat transfer coefficients. Here, heat transfer measurements for 0.2% Carbopol solution are presented. The evolution of the local and averaged heat transfer coefficients as function of Re' is discussed.

Fig. 7a shows for a 0.2% Carbopol solution, the evolution of the wall temperature, Θ_w , along the heating zone for different Re' from laminar to turbulent regime. The corresponding evolution of the Nusselt number is represented in Fig. 7b. For $Re' \leq 3000$, the flow is laminar and the experimental results are well described by the theoretical laminar solutions (11) and (7). For $Re' = 3200$ and

$x/D \leq 20$, the wall temperature increases according to (11), then departs from the theoretical laminar solution and remains constant from $x/D = 40$ until the exit of the heating zone. This is a typical effect of the transitional flow from laminar to turbulent regime. Near the entrance of heating zone, the thermal boundary layer is very thin and confined inside the viscous-sublayer. It grows radially according to the molecular diffusivity. But, when its thickness reach the turbulent core, its growth is stopped by the turbulent diffusivity. Consequently, the heat transfer coefficient and the wall temperature remain constant. It is also interesting to note that the thermal entrance length reduces drastically when Re' increases from 3000 to 3200. For higher Re' , the spreading velocity of a turbulent spot increases, the entrance length becomes shorter, the level of the plateau of Θ_w is lower and therefore the plateau for Nu is larger. This occurs because of increased eddy diffusion which moves the effective thermal region closer to the wall. Thus in the fully developed turbulent region, the temperature profile across the pipe becomes almost flat and the temperature gradient at the wall large, so that it requires only a short distance for the fluid to establish this kind of profile.

In Fig. 8, the local Nu vs. Re' for 0.2% Carbopol is represented for different positions from the entrance of the heated pipe. As expected the laminar heat transfer is sensitive to the position and varies as $Re'^{1/3}$. The critical Re' for transition in isothermal situation (2700) and when a wall constant heat flux is applied (3000) are almost the same (at least in the uncertainty domain). This results agree with Thomas [24]. For the 2% CMC solution, we found similar results. The main effect of non-Newtonian fluids is that the transition process takes place with a delay and in a larger range of Reynolds number. Finally, one has to retain that the heat transfer is governed by the dynamics of the flow.

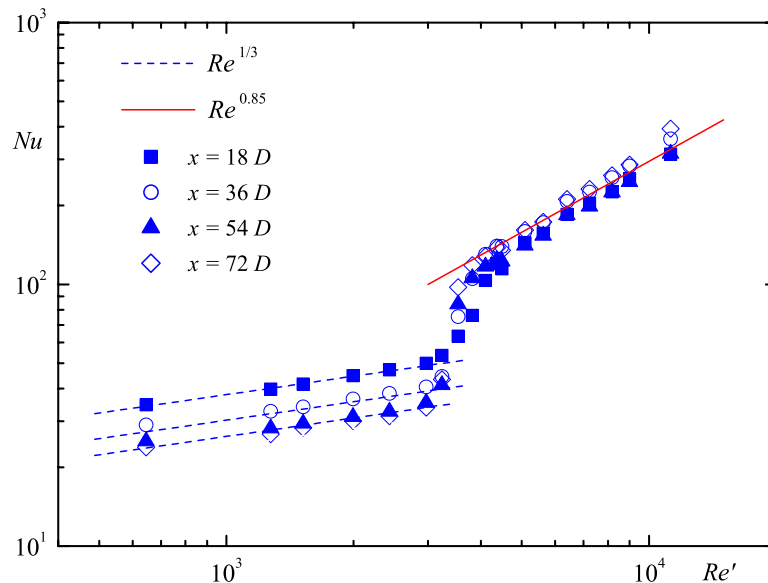


Fig. 8. Local heat transfer, Nu , as a function of Re' . The wall boundary condition is a constant heat flux ($\phi_w = 15.5 \text{ kW m}^{-2}$). The behaviour of the 0.2% Carbopol solution is described by the Herschel–Bulkley model (with $\tau_Y = 6.3 \text{ Pa}$, $K = 2.37 \text{ Pa s}^n$ and $n = 0.5$). The lines are $Re'^{1/3}$ and $Re'^{0.85}$ fits to guide the eyes.

5. Conclusions

We have performed a study of the heat transfer of a non-Newtonian fluid (0.2% Carbopol aqueous solution) in heated pipe flow. Rheological measurements indicate that the fluid is well described by a Herschel–Bulkley model of which the consistency decreases with the temperature. Isothermal developed pipe flow enters a heated pipe where the wall provides a heat flux. The flow was monitored using pressure drop and wall temperature along the pipe.

In laminar regime, heat transfer is well described by an extension of the L ev eque model, which take into account the non-Newtonian character and the variation of the consistency with the temperature.

Additional results using Newtonian fluids and shear thinning fluids indicate that, in pipe flow, transition to turbulence for non-Newtonian fluids is delayed. The results also show that the shear thinning as well as the yield stress increases the stability of the flow. In our experiments, the critical Reynolds numbers for the transitional regime in heated and isothermal flow are similar. This indicates that the heat transfer is governed by the dynamics of the flow. Moreover, temperature measurement along the pipe in transitional regime can increase drastically. Quantitative estimates as well as evolution of the heat transfer coefficient are provided.

Acknowledgements

The authors would like to thank C. Nouar for helpful discussion and rereading of the manuscript and Schlumberger for financial support.

Appendix A. Fully developed isothermal velocity profile and Metzner and Reed [33] Reynolds number for a Herschel–Bulkley fluid

Using, the radius, R , of the pipe as a characteristic scale length and the bulk velocity, U , as a characteristic scale velocity, it can be shown that for one dimensional shear flow we have [36,19]:

$$\frac{u}{U} = \begin{cases} \frac{n}{n+1} \left(\frac{Hb}{a}\right)^{\frac{1}{n}} (1-a)^{\frac{n+1}{n}}; & 0 \leq r \leq a \\ \frac{n}{n+1} \left(\frac{Hb}{a}\right)^{\frac{1}{n}} \left[(1-a)^{\frac{n+1}{n}} - (r-a)^{\frac{n+1}{n}} \right]; & a \leq r \leq 1 \end{cases} \quad (12)$$

Hb is the Herschel–Bulkley number (the ratio of the yield stress τ_Y to a nominal shear stress $K(U/R)^n$). The dimensionless radius, a , of the plug zone depends only on Hb and n . Using the continuity equation in integral form, we obtain:

$$0 = (1-a)^{3+m} - (3+m)(1-a)^{2+m} + \frac{(2+m)(3+m)}{2} (1-a)^{1+m} - \frac{(3+m)(2+m)(1+m)}{2} \left(\frac{a}{Hb}\right)^m, \quad (13)$$

where $m = 1/n$.

Re' for a Herschel–Bulkley fluid flow in a pipe is defined by $fRe' = 16$, where f is the Fanning friction factor. It can be shown that:

$$Re' = \frac{\rho U^{2-n'} D^{n'}}{8^{n'-1} k'}, \quad (14)$$

$$n' = \frac{(1-a) + \frac{2a(1-a)(1+m)}{2+m} + \frac{(1-a)^2(1+m)}{3+m}}{m+1-3(1-a) \left[a^2 + \frac{2a(1-a)(1+m)}{2+m} + \frac{(1-a)^2(1+m)}{3+m} \right]}, \quad (15)$$

$$k' = \left(\frac{K^m}{4}\right)^{n'} \left(\frac{\tau_Y}{a}\right)^{1-n'm} \left\{ (1-a)^{1+m} \left[1 + \frac{2(1-a)(1+m)}{a(2+m)} + \frac{(1-a)^2(m+1)}{a^2(3+m)} \right] \right\}^{-n'}. \quad (16)$$

Expressions for n' and k' depend on the Herschel–Bulkley model parameters and the radius of the plug, a , obtained by resolving Eq. (5). Koziki et al. [40] determined n' and k' for several rheological models and ducts arbitrary cross section.

References

- [1] I.J. Wygnanski, F.H. Champagne, On the transition in a pipe. Part. 1. The origin of puff and slugs and the flow in a turbulent slug, *J. Fluid Mech.* 59 (1973) 281–351.
- [2] A.J. Ghajar, L.-M. Tam, Flow regime map for horizontal pipe with uniform wall heat flux and three inlet configurations, *Exp. Therm. Fluid Sci.* 10 (1995) 287–297.
- [3] S.W. Churchill, Comprehensive correlating equations for heat, mass and momentum transfer in fully developed flow in smooth tubes, *Ind. Eng. Chem. Fund.* 16 (1) (1977) 109–116.
- [4] C. Nouar, I.A. Frigaard, Nonlinear stability of Poiseuille flow of a Bingham fluid: theoretical results and comparison with phenomenological criteria, *J. Non-Newtonian Fluid Mech.* 100 (2001) 127–149.
- [5] I. Frigaard, C. Nouar, On 3-dimensional linear stability of Poiseuille flow of Bingham fluids, *Phys. Fluids* 15 (10) (2003) 2843–2851.
- [6] M.P. Escudier, F. Presti, Pipe flow of a thixotropic liquid, *J. Non-Newtonian Fluid Mech.* 62 (1996) 291–306.
- [7] J. Peixinho, C. Nouar, C. Desaubry, B. Th eron, Laminar transitional and turbulent flow of yield stress fluid in a pipe, *J. Non-Newtonian Fluid Mech.* 128 (2005) 172–184.
- [8] F.T. Pinho, J.H. Whitelaw, Flow of non-Newtonian fluids in a pipe, *J. Non-Newtonian Fluid Mech.* 34 (1990) 129–144.
- [9] M.P. Escudier, F. Presti, S. Smith, Drag reduction in the turbulent pipe flow of polymers, *J. Non-Newtonian Fluid Mech.* 81 (1999) 197–213.
- [10] M. Rudman, H.M. Blackburn, L.J.W. Graham, L. Pullum, Turbulent pipe flow of shear-thinning fluids, *J. Non-Newtonian Fluid Mech.* 118 (2004) 33–48.
- [11] I.C. Walton, S.H. Bittleston, The axial flow of a Bingham plastic in a narrow eccentric annulus, *J. Fluid Mech.* 222 (1991) 39–60.
- [12] E. Hirai, Theoretical explanation of heat transfer in the laminar region of a Bingham fluid, *A.I.Ch.E. J.* 5 (1959) 130–133.
- [13] E.H. Wissler, R.S. Schechter, The Graetz–Nusselt problem (with extension) for a Bingham plastic, *Chem. Eng. Prog. Symp. Ser.* 29 (55) (1959) 203–208.
- [14] B.F. Blackwell, Numerical solution of the Graetz problem for a Bingham plastic in laminar tube flow with constant wall temperature, *ASME J. Heat Transfer* 107 (5) (1985) 466–468.
- [15] P.R. Johnston, Axial conduction and the Graetz problem for a Bingham plastic in laminar tube flow, *Int. J. Heat Mass Transfer* 34 (1991) 1209–1217.
- [16] T. Min, J.Y. Yoo, H. Choi, Laminar convective heat transfer of a Bingham plastic in a circular pipe-I. Analytical approach-thermally fully developed flow and thermally developing flow (the Graetz

- problem extended), *Int. J. Heat Mass Transfer* 40 (13) (1997) 3025–3037.
- [17] T. Min, J.Y. Yoo, Laminar convective heat transfer of a Bingham plastic in a circular pipe with uniform wall heat flux: The Graetz problem extended, *ASME J. Heat Transfer* 121 (8) (1999) 556–563.
- [18] G. Forrest, W.L. Wilkinson, Laminar heat transfer to temperature-dependent Bingham fluids in tubes, *Int. J. Heat Mass Transfer* 16 (1973) 2377–2391.
- [19] C. Nouar, R. Devienne, M. Lebouché, Convection thermique pour un fluide de Herschel-Bulkley dans la région d'entrée d'une conduite, *Int. J. Heat Mass Transfer* 37 (1) (1994) 1–12.
- [20] M. Soares, M.F. Naccache, P.R. Souza-Mendes, Heat transfer to viscoplastic materials flowing laminarily in the entrance region of tubes, *Int. J. Heat Fluid Flow* 20 (1999) 60–67.
- [21] N. Patel, D.B. Ingham, Analytic solutions for the mixed convection flow of non-Newtonian fluids in parallel plate ducts, *Int. Comm. Heat Mass Transfer* 21 (1) (1994) 75–84.
- [22] N. Patel, D.B. Ingham, Mixed convection flow of a Bingham plastic in an eccentric annulus, *Int. J. Heat Fluid Flow* 15 (2) (1994) 132–141.
- [23] C. Nouar, Thermal convection for a thermo-dependent yield stress fluid in an axisymmetric horizontal duct, *Int. J. Heat Mass Transfer* 48 (25–26) (2005) 5520–5535.
- [24] D.G. Thomas, Heat and momentum transport characteristics of non-Newtonian aqueous Thorium Oxide suspensions, *A.I. Ch. E.J.* 6 (1960) 631–639.
- [25] S.S. Yoo, Heat transfer and friction factors for non-Newtonian fluids in fluids in turbulent pipe flow, Ph.D. Department of Energy Engineering, University of Illinois, (1974).
- [26] G.P. Roberts, H.A. Barnes, New measurements of the flow-curves for Carbopol dispersions without slip artefacts, *Rheol. Acta* 40 (2001) 499–503.
- [27] J.-Y. Kim, J.-Y. Song, E.-J. Lee, S.-K. Park, Rheological properties and microstructures of Carbopol gel network system, *Colloid. Polym. Sci.* 281 (2003) 614–623.
- [28] M.P. Escudier, I.W. Gouldson, A.S. Pereira, F.T. Pinho, R.J. Poole, On the reproducibility of the rheology of shear-thinning liquids, *J. Non-Newtonian Fluid Mech.* 97 (2001) 99–124.
- [29] M. Maïmi, R. Devienne, M. Lebouché, Etude dynamique et thermique de l'écoulement de Couette Taylor-Poiseuille : Cas d'un liquide présentant un seuil d'écoulement, *Int. J. Heat Mass Transfer* 33 (1990) 381–391.
- [30] T. Loulou, H. Peerhossaini, J.P. Bardon, Etude expérimentale de la conductivité thermique de fluides non-Newtoniens sous cisaillement application aux solutions de Carbopol 940, *Int. J. Heat Mass Transfer* 35 (10) (1992) 2557–2562.
- [31] H.A. Barnes, J.F. Hutton, K. Walters, *An introduction to rheology*, Elsevier, Amsterdam, 1989.
- [32] W.Y. Lee, Y.I. Cho, J.P. Hartnett, Thermal conductivity measurements of non-Newtonian fluids, *Lett. Heat Mass Transfer* 8 (1981) 255–259.
- [33] A.B. Metzner, J.C. Reed, Flow of non-Newtonian fluids-correlation of laminar transition and turbulent-flow regions, *A.I. Ch. E. J.* 1 (1955) 433–435.
- [35] J.T. Park, R.J. Mannheimer, T.A. Grimley, T.B. Morrow, Pipe flow Measurement of a transparent non-Newtonian slurry, *J. Fluids Eng.* 111 (1989) 331–336.
- [36] R.B. Bird, G.C. Armstrong, O. Hassager, *Dynamics of polymer liquids*, vol. 1, Wiley, 1977.
- [37] A. Bejan, *Convection heat transfer*, Wiley, 1984.
- [38] H. Ockendon, J.R. Ockendon, Variable viscosity flows in heated and cooled channels, *J. Fluid Mech.* 83 (1977) 177–190.
- [39] S.M. Richardson, Flow of variable viscosity fluids in ducts with heated walls, *J. Non-Newtonian Fluid Mech.* 25 (1986) 137–156.
- [40] W. Koziicki, C.H. Chou, C. Tiu, Non-Newtonian flow in ducts of arbitrary cross-section shape, *Chem. Eng. Sci.* 21 (1966) 665–679.